Organic & Biomolecular Chemistry

PAPER

View Article Online
View Journal | View Issue

Cite this: Org. Biomol. Chem., 2017, 15, 9008

Cationic phthalocyanine dendrimers as potential antimicrobial photosensitisers†

Rubén Ruiz-González, [a] Francesca Setaro, [b] Òscar Gulías, [a] Montserrat Agut, [a] Uwe Hahn, *[b,c] Tomás Torres *[b,d,e] and Santi Nonell *[a]

Received 10th September 2017,
Accepted 9th October 2017

DOI: 10.1039/c7ob02270k

rsc.li/obc

In the present study we describe the synthesis, photophysical properties and the photoinactivation performance against representative microorganisms of two families of cationic dendrimeric phthalocyanines as potential photosensitisers. Four charged dendrimeric compounds varying in their degree of ionicity (4 or 8 positive charges) and the coordinating metal (zinc or ruthenium) are compared and assessed as potential photosensitising agents in terms of their antimicrobial activity.

Introduction

Pathogenic microorganisms have become a universal threat and leading cause of mortality and morbidity worldwide.[1–6] The issue of prevention and control of infectious diseases continues to be open and a series of highly virulent pathogens are emerging in and beyond hospital settings.[7,8] Concomitant with the rise of antibiotic-resistant bacteria, the approval of new antibiotics has slowed dramatically. Moreover, the number of novel compounds with new mechanisms of action remains scarce, despite the efforts devoted to finding new hits among emerging drugs.[9–11] Thus, the development of novel approaches to address this problem has become urgent.[12] Several alternatives to antibiotic treatments have gained attraction recently.[13–19] Some of them, including photodynamic therapy,[20,21] are not novel, but their use was eclipsed mainly due to two reasons: insufficient understanding among researchers at the moment of their discovery and the advent of antibiotics.

Photodynamic therapy (PDT) consists of an adequate combination of three factors: light, oxygen and a light-active compound referred to as a photosensitiser (PS). None of them are toxic *per se*; however, their combination leads to the formation of highly reactive oxygen species (ROS) such as singlet oxygen ($^1O_2$) responsible for exerting cytotoxic damage.[20] The advantages of antimicrobial PDT (aPDT) over traditional antibiotics include the activity against antibiotic-resistant species and the lack of development of resistance due to its multitarget mode of action. These attributes make aPDT suitable for the treatment of superficial and localised infectious diseases.[20–22]

Phthalocyanines (Pcs) have been investigated in detail for many years due to their interesting physical properties.[23–27] This family of compounds have also become popular for PDT applications, especially for cancer treatment, since Pc derivatives including some metal core atoms such as zinc, ruthenium or silicon display photosensitising activity.[28–35] However, due to their highly hydrophobic nature, Pcs require suitable functionalisation or combination with carrier systems to ensure appropriate administration within a therapy. Dendrimer-encased PSs are an attractive option to achieve successful biomedical applications[36] because their inner chromophores are partially shielded from media. This allows maintaining their photoactive form since the bulky substituents prevent the aggregation of the macrocycle. Moreover, their large dimensions allow extended circulation in the blood and higher accumulation of dendronised PSs in the tumour tissues *via* the so-called enhanced permeation retention effect.[37] Several series of Pc-based architectures and their ability to generate $^1O_2$ have been previously described.[35,38–41] However, to our knowledge, cationic dendrimeric Pcs have not been studied for antimicrobial purposes. Thus, this work explores the synthesis, photophysical characterisation and potential application of ruthenium- and zinc-Pcs encased in multi-cationic dendrimers as a potential PS platform for aPDT.

[a]Institut Químic de Sarriá, Universitat Ramon Llull, Barcelona, Spain. E-mail: santi.nonell@iqs.url.edu; Fax: +34 932 056 266; Tel: +34 932 672 000
[b]Departamento de Química Orgánica, Universidad Autónoma de Madrid, Cantoblanco, 28049 Madrid, Spain. Fax: +34 91497 3966; Tel: +34 91497 4151
[c]Laboratoire de Chimie des Matériaux Moléculaires, Université de Strasbourg et CNRS (UMR 7509), Ecole Européenne de Chimie, Polymères et Matériaux (ECPM), 25 rue Becquerel, 67087 Strasbourg Cedex 2, France. Fax: +33 368 85 27 64; Tel: +33 368 85 27 64
[d]IMDEA-Nanociencia, c/ Faraday, 9, Cantoblanco, 28049 Madrid, Spain
[e]Institute for Advanced Research in Chemical Sciences (IAdChem), Universidad Autónoma de Madrid, 28049 Madrid, Spain

†Electronic supplementary information (ESI) available: NMR spectra and MS files of the phthalonitriles and phthalocyanines. See DOI: 10.1039/c7ob02270k

Results and discussion

Synthesis description

The synthesis started with the preparation of dimethylamino-appended phthalonitrile **1**, which confers the basic motif of terminal moieties that can be found in the dendritic phthalonitriles described thereafter. In first instance, **1** has been prepared from 4-nitrophthalonitrile and dimethylaminoethanol (DMAE) following a literature protocol.[42,43] However, it turned out that the use of microwave-assisted irradiation gave **1** in shorter time with easier purification and a higher yield. This rather simple 1,2-benzenedicarbonitrile was then engaged in the literature-described cyclotetramerisation in the presence of $Zn(OAc)_2$ under the formation of **2**.[42,43] Likewise, the presence of $RuCl_3{\cdot}3H_2O$ as the metal template for the formation of the Pc macrocycle allowed obtaining **3** in almost quantitative yield. Of note, pyridine has been added to the reaction medium as two equivalents of these N-type ligands occupy the axial positions. The coordination of two pyridine ligands at the axial positions is very important at the stage of evaluating the experimental data as this coordination prevents to a great extent the aggregation often encountered for Pcs. In contrast, the aggregation phenomenon has to be considered important in the case of zinc Pcs as the axial positions are not occupied by ligands. Both Pcs were then subjected to an excess of methyl iodide to give the respective quaternary ammonium salts in very high yields as a dark green solid in the case of **ZnPc** or **RuPc** as a blue solid (Scheme 1).

The quaternisation of **2** has been described in the literature.[42,43] It is important to note that we were aiming at quaternary ammonium salts resulting from the alkylation of terminal amines rather than simple protonation. This is especially important when introducing the dendrimer polyelectrolytes into physiological media as the stability of the former is by far higher when compared to the latter. Depending on the pH prevalent in the corresponding part of the body, the proton might be abstracted under formation of neutral species, which might then lead to an undesired precipitation due to decreased hydrophilicity.

While attempting to construct fractal dendritic wedges containing an increasing amount of dimethylaminoethyl end groups, the respective coupling reactions proved inefficient or/and the purification too tedious. Consequently, this prompted us to realign the synthetic strategy to prepare phthalonitriles endowed with Boc-protected amino groups rather than employing the dimethylamino terminal units. The simple benzenedicarbonitrile derivative **4** has been synthesised again by *ipso*-substitution of 4-nitrophthalonitrile and 2-(*tert*-butoxycarbonyl)aminoethanol according to a described method.[44] On the other hand, compound **5** has been easily prepared closely following the procedure of Liskamp *et al.*[45,46]

This building block contains two Boc protected ethoxyamino groups in positions **3** and **5** and a carboxylic acid function prone to amide coupling reactions. Accordingly, **4** has been deprotected under the use of trifluoroacetic acid (TFA) and after neutralization subjected to benzotriazol-1-yloxytripyrrolidinophosphonium hexafluorophosphate (PyBOP)-mediated amide bond formation. The first generation derivative **6** has been obtained in 95% yield as colourless foam. Iterative deprotection of the two Boc protection groups was performed again by PyBOP-assisted amidation reactions which then readily provided the second generation phthalonitrile **7** with four terminal Boc-protected amino groups in 83% yield as a colourless solid (Scheme 2).

Similarly to the synthesis of Pcs **2** and **3**, phthalonitriles **4**, **6** and **7** were engaged in the cyclotetramerisation in either the presence of $Zn(OAc)_2$ or a mixture of $RuCl_3{\cdot}3H_2O$ and pyridine. However, only the respective zinc Pcs **8**[47]–**9** and ruthenium Pcs **11**–**12** have been obtained as dark green or dark blue solids after purification by column chromatography and size exclusion chromatography. The second generation derivative **10** has been obtained in very small quantities and mass spectroscopic characterization indicated the target peak, but due to the small amount of the compound, quaternisation has not been attempted. Similarly, the synthesis of the second generation ruthenium Pc was found to give inseparable mixtures of compounds regardless of the applied reaction conditions most likely due to steric hindrance hampering the formation of the desired Pc. At the last stage of the synthetic sequence, again a two-step protocol has been employed for the quaternisation of the terminal amino groups, *i.e.* (i) cleavage of the Boc groups by TFA and (ii) alkylation with a mixture of 1,2,2,6,6-pentamethylpiperidine (PMP) and CH_3I (Scheme 3).[48]

The polycationic zinc Pcs **ZnPc** and **ZnPc1** as well as the ruthenium Pcs **RuPc** and **RuPc1** have been obtained in high yields after repetitive sonication/filtration steps from various

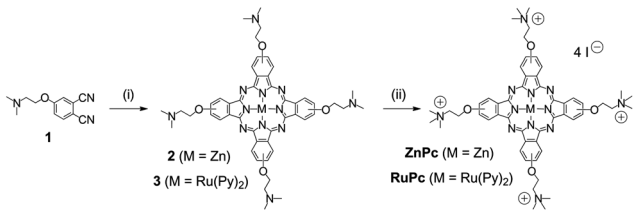

Scheme 1 Synthetic route to zero generation tetracationic **ZnPc** and **RuPc**. Reagents and conditions: (i) **2**: $Zn(OAc)_2$, DMAE, reflux, overnight, 21%; **3**: $RuCl_3{\cdot}3H_2O$, pyridine, DBU, ethoxyethanol, reflux, overnight, 24%; (ii) MeI, DMF, 40 °C, 6 h (**ZnPc**: 65%, **RuPc**: 97%).

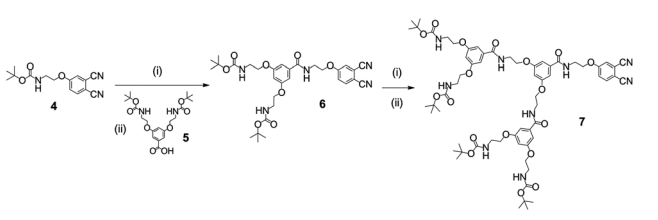

Scheme 2 Synthetic route to second generation Boc-terminated phthalonitrile **7**. Reagents and conditions: (i) TFA, CH_2Cl_2, 0 °C to room temperature (**6**: 3 h, **7**: 4 h); (ii) PyBOP, NEt_3, room temperature, overnight (**6**: 95%, **7**: 83%).

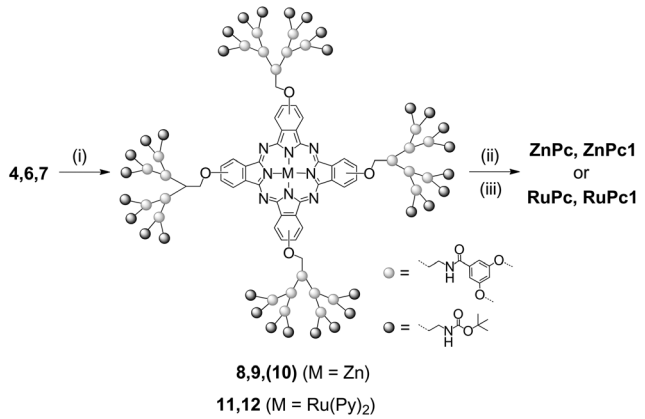

Scheme 3 Synthetic route to second generation zinc and ruthenium Pcs. Reagents and conditions: (i) **8–10**: $Zn(OAc)_2$, DMAE, reflux, overnight (**8**: 45%, **9**: 33%, **10**: 2%); **11–12**: $RuCl_3{\cdot}3H_2O$, pyridine, DBU, ethoxyethanol, reflux, overnight, (**11**: 7%, **12**: 7%); (ii) TFA, CH_2Cl_2, 0 °C to room temperature (**ZnPc**, **RuPc**, **RuPc1**: 4 h, **ZnPc1**: 7 h); (iii) PMP, MeI, DMF, room temperature, overnight (**ZnPc**: 98%, **ZnPc1**: 80%, **RuPc**: 86%, **RuPc1**: 70%).

solvents. As expected, the series of multiply charged Pcs showed good solubility in polar media including water.

Photophysical characterisation

Fig. 1 shows the normalised absorption spectra of all four polycationic Pcs in tetrahydrofuran (THF), water and dimethylsulfoxide (DMSO). Marked changes are observed depending on the extent of aggregation that they experience in each solvent. Aside from minor peak shifts derived from solvatochromic effects, important changes are evidenced in terms of different relative intensities of the bands in the Soret and Q regions. The spectrum in DMSO is taken as representative of the monomeric form, characterised by a narrow and intense red Q band.[37] The general trend is that the dendrimeric Pcs tend to disaggregate in aqueous media. This is not fully true for compound **ZnPc** (panel a in Fig. 1) whose Soret band, but not the Q band, resembles that in DMSO. Both ruthenium derivatives

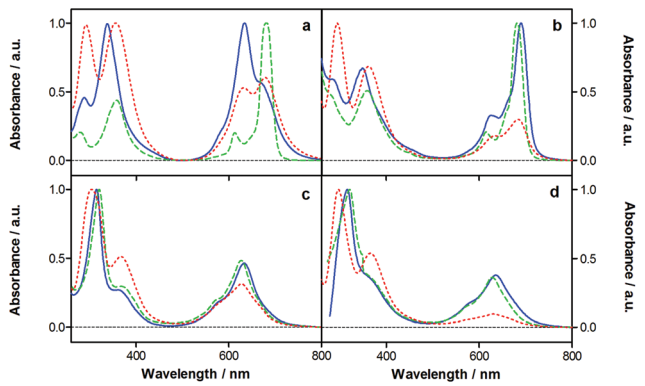

Fig. 1 Normalised absorption spectra of dendrimeric cationic phthalocyanines in DMSO (green dashed line), THF (red dotted line) and water (blue solid line). **ZnPc** (a), **ZnPc1** (b), **RuPc** (c) and **RuPc1** (d).

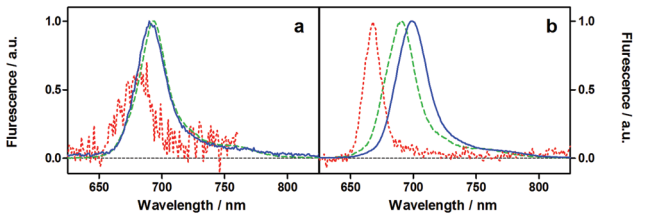

Fig. 2 Normalised fluorescence spectra of dendrimeric cationic zinc-Pcs in DMSO (green dashed line), THF (red dotted line) and water (blue solid line). **ZnPc** (a), **ZnPc1** (b).

disaggregate almost completely in water. Despite having the same charges as their zinc analogues, the presence of the apical pyridyl groups seems to prevent aggregation.

The fluorescence of the compounds was also studied using the same series of solvents. As observed in Fig. 2 and Table 1, there is a substantial difference in the behaviour depending on the nature of the central metal ion, only ZnPcs being fluorescent.

Moreover, a major difference in the fluorescence quantum yield values (Φ_F) was also encountered depending on the medium, once again attributed to aggregation effects. Especially significant is the case of **ZnPc1** that exhibits Φ_F values two orders of magnitude lower in THF than in water (Table 1).

Finally, the ability of the Pcs to sensitise the production of $^1O_2$ was studied both in THF and in deuterated aqueous media. The quantification of the $^1O_2$ quantum yield (Φ_Δ) was performed by direct observation of $^1O_2$ phosphorescence at 1275 nm (Fig. 3) exciting either at 355 nm (for zinc-Pcs) or at 532 nm (for ruthenium-Pcs). In line with fluorescence results, the photosensitising properties of the Pcs correlated with the extent of aggregation, being more efficient when less aggregated. This effect was especially noticeable for compound **ZnPc1** whose Φ_Δ value in deuterated water was almost two orders of magnitude higher than in THF (Table 1). As regards $^1O_2$ decay kinetics (monitored through the $^1O_2$ lifetime value, τ_Δ), ruthenium-Pc dendrimers manifest $^1O_2$ self-quenching. This is evidenced from the fact that their $^1O_2$ lifetime values are shorter than those reported in the literature for the neat solvents (21 μs in THF and 65 μs in D_2O, respectively).[49] This effect has previously been observed for other ruthenium dendrimeric derivatives, although to a lesser extent.[35]

As compared to other dendrimeric Pcs, the reported cationic ZnPcs outperform poly-anionic analogues in terms of production of $^1O_2$ in aqueous media.[38] Regarding novel cationic ruthenium-Pcs, their $^1O_2$ sensitising capacity remains similar to that reported for other anionic dendrimeric analogues.[35,39]

Photoinactivation studies

The incorporation of positive charges in PSs has been a benchmark in the re-emerging of aPDT as a potential platform to fight antibiotic-resistant microorganisms.[52–56] We have assessed for the first time the potential of four different cat-

Table 1 Summary of the photochemical properties of the dendrimeric phthalocyanines of study in water (D_2O for Φ_Δ measurements) and THF (values in parentheses)

Compound	λ_{Abs} [a]/nm	Φ_F [b]	Φ_Δ [c]	τ_Δ /μs
ZnPc	634 (679)	0.035 (<1×10^{-4})	0.022 (0.002)	62.8 (20.8)
ZnPc1	690 (684)	0.538 (0.002)	0.119 (0.004)	64.0 (21.0)
RuPc	633 (628)	<1×10^{-3} (<1×10^{-4})	0.015 (0.011)	45.3 (19.7)
RuPc1	636 (631)	<1×10^{-3} (<1×10^{-4})	0.017 (0.001)	38.7 (19.4)

[a] Maximum wavelength at the Q-band. [b] Rhodamine 6G as the reference (Φ_F (ethanol) = 0.94).[50] [c] 5,10,15,20-Tetraphenyl-21H,23H-porphine (TPP; Φ_Δ (THF) = 0.62 and *meso*-tetrakis(4-sulfonatophenyl)-porphyrin (TPPS; Φ_Δ (D_2O) = 0.64 as references.[51]

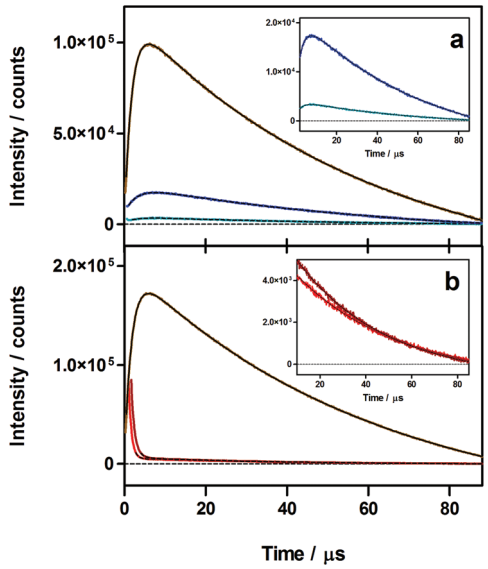

Fig. 3 Time-resolved near-infrared $^1O_2$ phosphorescence signals at 1275 nm in air-saturated D_2O solutions for [a] **ZnPc** (green) & **ZnPc1** (blue) and [b] **RuPc** (red) & **ZnPc1** (garnet). TPPS was used as the reference (brown). Dashed lines represent datasets from signal fitting. Inset: Magnification of the $^1O_2$ signals of the cationic Pcs.

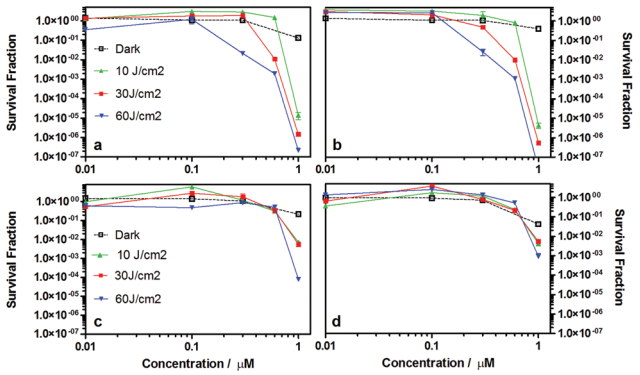

Fig. 4 *S. aureus* photoinactivation studies with **ZnPc** (a), **ZnPc1** (b), **RuPc** (c) and **RuPc1** (d) upon red light irradiation. Light doses: 10 J cm^{-2} (triangles), 30 J cm^{-2} (filled squares), and 60 J cm^{-2} (inverted triangles). Working concentrations: 0.01, 0.1, 0.3, 0.6 and 1 μM. Dark controls are represented with empty squares. Results are the mean from at least three different experiments.

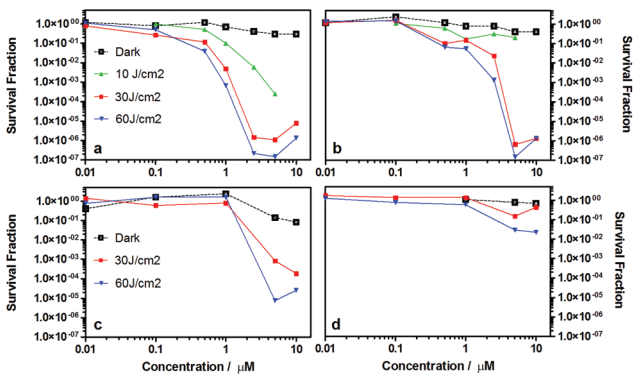

Fig. 5 *E. coli* photoinactivation studies with **ZnPc** (a), **ZnPc1** (b), **RuPc** (c) and **RuPc1** (d) upon red light irradiation. Light doses: 10 J cm^{-2} (triangles), 30 J cm^{-2} (filled squares), and 60 J cm^{-2} (inverted triangles). Working concentrations: 0.01, 0.1, 0.5, 1, 2.5, 5 and 10 μM. Dark controls are represented with empty squares. Results are the mean from at least three different experiments.

ionic dendrimeric Pcs as potential antimicrobial PSs. Zinc and ruthenium Pcs encased in multi-cationic dendrimers were assayed against representative members of Gram-positive (*Staphylococcus aureus*), Gram-negative (*Escherichia coli*) and fungi (*Candida albicans*) to assess their potential use as broad-spectrum photosensitising agents (Fig. 4–6).

Fig. 4 presents photoinactivation results against *S. aureus* upon different PS concentrations and light-doses. Two different trends are revealed out of the figure: (i) Both zinc-coordinated Pcs are capable of achieving over 6-$\log_{10}$ colony forming units per millilitre (CFU mL^{-1}) reduction at 1 μM for the higher light-doses and a bactericidal effect (3-$\log_{10}$ CFU mL^{-1} reduction) when irradiating at 60 J cm^{-2} with a concentration of 0.6 μM. Overall photo-killing efficiency is slightly higher for the octacationic **ZnPc1** as compared to the **ZnPc** performance, especially at the highest concentration assayed. (ii) Ruthenium-coordinated compounds have resulted less harmful against *S. aureus* achieving the bactericidal effect only in the case of maximum concentration and light dose (namely, 1 μM and 60 J cm^{-2}). Octacationic **RuPc1** is slightly less efficient than its tetracationic analogue. Non-irradiated samples (dark controls) reveal that at maximum concentration

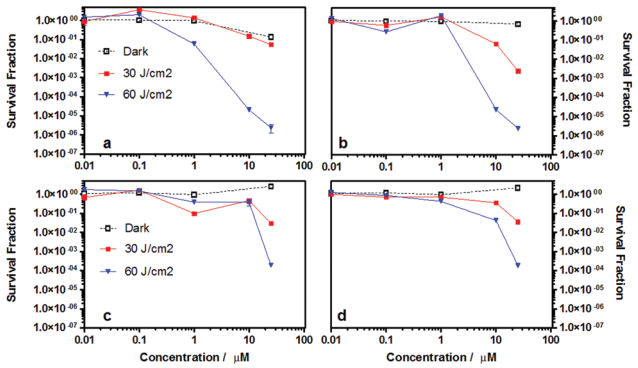

Fig. 6 *C. albicans* photoinactivation studies with **ZnPc** (a), **ZnPc1** (b), **RuPc** (c) and **RuPc1** (d) upon red light irradiation. Light doses: 30 J cm^{-2} (filled squares), and 60 J cm^{-2} (inverted triangles). Working concentrations: 0.01, 0.1, 1, 10 and 25 μM. Dark controls are represented with empty squares. Results are the mean from at least three different experiments.

there is an apparent 1-$\log_{10}$ CFU mL^{-1} reduction inherent to drug toxicity. This dark toxicity especially affects the **RuPc1** compound, which is poorly efficient.

As for *E. coli* photoinactivation results, Fig. 4 shows the behaviour of the four cationic dendrimers upon different light and concentration conditions. The dark toxicity was below 1-$\log_{10}$ CFU mL^{-1} reduction for **ZnPc**, **ZnPc1** and **RuPc1**, but higher for **RuPc** at concentrations above 5 μM. A remarkable difference in the photodynamic inactivation efficiency was also observed depending on the coordinated metal. Zinc-coordinated dendrimers exhibited a photokilling performance far better than their ruthenium analogues. Reductions over 6-$\log_{10}$ CFU mL^{-1} were achieved at concentrations as low as 2.5 μM for **ZnPc** and 5 μM for **ZnPc1** at 30 J cm^{-2} light dose. In contrast, a lower photoinactivation was obtained when using **RuPc** even under harsher photodynamic conditions (approximately 5-$\log_{10}$ reduction with 5 μM and 60 J cm^{-2}, but with a higher dark toxicity). Finally, **RuPc1** only accomplished a modest 2-$\log_{10}$ CFU mL^{-1} reduction even under conditions as high as 50 μM and 100 J cm^{-2} (data not shown). Of note, the inactivation efficiency slightly decreased in some cases when increasing from 5 to 10 μM and at high light-doses. This behaviour might be attributed to increased aggregation under these experimental conditions.

Finally, photodynamic inactivation studies were also performed against *C. albicans* as a representative opportunistic fungal pathogen. As in the previous scenarios, the dendrimeric cationic zinc-Pcs outperformed the ruthenium analogues in terms of reducing cell viability upon comparable light/dose conditions. While **ZnPc** and **ZnPc1** were capable of achieving approximately 6-$\log_{10}$ CFU mL^{-1} reduction, **RuPc** and **RuPc1** yielded a reduction in CFU mL^{-1} two-orders of magnitude inferior. In all cases, the concentration required to exert a noticeable damage was higher as compared to the studies with bacteria.[57] In terms of charges, minor differences arise when comparing the photokilling efficiency of the tetracationic *versus* octacationic dendrimers in both series of compounds. For the low light-dose conditions, octacationic compounds seem to respond more efficiently; however, this differences vanish at 60 J cm^{-2} light-dose, both for ruthenium- and zinc-Pcs. Of note, octacationic **RuPc1** was capable of exerting almost 4-$\log_{10}$ CFU mL^{-1} reduction against this fungi model, despite being poorly phototoxic against both bacterial models.

Overall, the results obtained in the photodynamic inactivation studies against all representative microorganisms correlate with their photophysical behaviour in solution. Hence, zinc-coordinated dendrimers have shown superior properties than the ruthenium counterparts for all three microbial models. This is especially noticeable comparing octacationic Pcs. Thus, in the concentration/light doses in which **ZnPc** and **ZnPc1** achieved microbial reduction over 6-$\log_{10}$ CFU mL^{-1}, dendrimeric ruthenium-Pcs were unable to achieve similar yields. Other ruthenium complexes have been reported to behave as antimicrobial agents,[58] pointing out that the lower efficiency has to do with the overall photophysics of the compounds rather than the capacity of the coordinated metal itself. Of note, for the zinc-coordinated derivatives, the photokilling efficiency – similar for both compounds – does not fully correlate with the measured Φ_Δ values in solution (**ZnPc1** is 2-fold higher in water and 5-fold higher in THF than **ZnPc**). Different extents of aggregation under the experimental conditions upon interaction with the different microorganisms may be responsible for this observation.

Previous studies have attempted to establish relationships between the photodynamic inactivation efficacy and the global charge of the PSs although with contradictory results. For instance, Merchat *et al.* described no differences in activity despite changes in the net charge.[59] On the other hand, the study of Caminos *et al.* showed that the photosensitising efficiency of a series of *meso*-substituted cationic porphyrins against *E. coli* followed the trend $(PS)^{3+} > (PS)^{4+} > > (PS)^{2+} > (PS)^{+}$ in terms of enhanced photoinactivation.[60] In another work, Alves *et al.* compared the bacterial photoinactivation process of seven cationic porphyrins with up to four positive charges for Gram-positive and Gram-negative bacteria.[61] The study showed that tri- and tetracationic porphyrins resulted more efficient than the less charged analogues, consistent with Caminos *et al.* Moreover, photokilling was dependent not only on the net number of positive charges, but also on the charge distribution and nature of substituent groups.[62] Studies with tricationic porphycenes (asymmetric porphyrin isomers) have shown a broad-spectrum activity and also slight differences depending on the peripheral substituent.[56,62] Herein, our results would point out that dendrimeric octacationic Pcs slightly outperform tetracationic analogues in solution, but do not show a clear improved photoinactivation performance overall. Further studies ought to be addressed to compare the effect of functional groups relative to the resulting photoinactivation performance.

Conclusion

Four different cationic dendrimeric Pcs have been synthesised with either zinc or ruthenium in the centre, fully characterised and compared against the representative microbial species (Gram-positive/Gram-negative bacteria and fungi) in order to correlate their photochemical behaviour in solution with their photokilling efficiency. The differences arising from the inner central metal lead to different behaviours in solution with zinc-compounds being much more efficient displaying higher $^1O_2$ yields in solution and, thus, obtaining a higher bacterial reduction upon irradiation. Finally, our results show that an increase of the net charge from four to eight positive charges does not have a marked impact in terms of photokilling efficiency despite exhibiting slightly better singlet oxygen production in solution. While overall promising, further studies should be addressed to optimise the final dendrimer candidates and also explore the possible effect of peripheral substituents.

Experimental section

Chemistry

General remarks. Chemicals were purchased from commercial suppliers and used without further purification. The synthesis of compounds **1**,[42,43] **2**,[42,43] **4**,[44] **5**,[45,46] **8**,[47] **ZnPc**[42,43] has been accomplished according to the literature procedures. Microwave reactions were carried out in CEM Discovery apparatus. Thin layer chromatography was carried out on aluminium sheets, pre-coated with silica gel 60 F254 (0.2 mm thick, E. Merck); visualisation was by UV-vis light. Column chromatography was performed on glass columns packed with silica gel, Merck-60 (230–400 mesh, 60 Å). Gel permeation chromatography (GPC) was performed using Bio-Beads S-X1 (200–400 mesh). NMR spectra were recorded at 25 °C on a BRUKER AC 300 (300 MHz) instrument with a solvent signal as the reference (H_{pc}: Pc protons, H_{pn}: phthalonitrile protons, H_{py}: pyridine protons, H_{ar}: aromatic protons). UV-vis spectra were recorded on a JASCO V-660 spectrophotometer. IR spectra were recorded on a Bruker Vector 22 spectrophotometer. HRMS spectra and MALDI-TOF mass spectra were recorded on a Bruker Reflex III spectrometer. Matrix-assisted laser desorption/ionization time-of-flight (MALDI-TOF) mass spectra were recorded in the positive ion mode with a Bruker Ultrareflex III TOFTOF spectrometer equipped with a Nd:YAG laser operating at 355. ESI (electrospray ionization) mass spectra were recorded with an Applied Biosystems QSTAR using as injection system HPLC1100 (Agilent Technologies).

Synthetic procedures

4-[(*N*,*N*-Dimethylamino)ethoxy]phthalonitrile (1). In a microwave tube, a mixture of 4-nitrophthalonitrile (1.00 g, 5.78 mmol) and DMAE (0.81 mL, 8.09 mmol) was dissolved in anhydrous DMF (10 mL). After stirring for 10 minutes, anhydrous potassium carbonate (3.20 g, 23.15 mmol) was added and the solution was heated for 25 min at 100 °C under microwave irradiation (300 W maximum power input). After cooling to room temperature, the mixture was transferred into a one-neck flask and the solvent was evaporated to dryness. The residue was partitioned between H_2O and CH_2Cl_2, the organic phase separated and the water phase was extracted with CH_2Cl_2. The combined organic phase was dried with $MgSO_4$ and the solvent was removed under reduced pressure. Gradient column chromatography (silica gel; eluent: CH_2Cl_2 to CH_2Cl_2/CH_3OH 8 : 1) gave **1** (1.09 g, 88%) as pale yellow viscous oil. The characterisation data confirmed the literature values.[43]

Preparation of ruthenium phthalocyanine 3. A mixture of **1** (300 mg, 1.39 mmol), $RuCl_3{\cdot}3H_2O$ (72 mg, 0.35 mmol), pyridine (226 μL, 2.79 mmol) and DBU (21 μL, 1.39 mmol) in ethoxyethanol (1.5 mL) was refluxed overnight. After cooling to room temperature, the volatiles were removed under reduced pressure and the crude was purified by column chromatography (neutral alumina; eluent: CH_2Cl_2/MeOH 10 : 1) followed by GPC (eluent: THF) to give **3** (382 mg, 98%) as a dark blue solid. M.p.: >250 °C; ^{1}H NMR (300 MHz, $CDCl_3$): δ = 2.50 (s, 24H, CH_3), 3.00 (br, 8H, CH_2N), 3.70 (br, 4H, H_{py}), 4.58 (br, 8H, CH_2O), 5.24 (br, 4H, H_{py}), 6.05 (t, 2H, H_{py}), 7.48 (m, 4H, H_{pc}), 8.61 (d, 4H, H_{pc}), 8.97 ppm (m, 4H, H_{pc}); FT-IR (film): ν = 2957, 2924, 2360, 1608, 1397, 1233 cm^{-1}; UV-vis (THF): λ_{max} (log ε) = 209 (4.7), 319 (4.6), 624 (4.3); ESI-MS (MeOH + 1% HCOOH): m/z $[M + H]^+$ calcd for $C_{58}H_{63}N_{14}O_4Ru$: 1121.4, found 1121.7; $[M + H (-2py)]^+$ calcd for $C_{48}H_{53}N_{14}O_4Ru$: 963.3, found 963.6.

Preparation of polycationic RuPc. Compound **3** (22 mg, 19.6 μmol) was dissolved in DMF (0.5 mL), CH_3I (49 μL, 0.786 mmol) was added and the reaction stirred at 40 °C for 6 h. After cooling to room temperature, the crude was precipitated in ether, the solid was filtered and washed with CH_2Cl_2, acetone, ethyl acetate and ether to give **RuPc** (32 mg, 97%) as a dark blue powder. ^{1}H NMR (300 MHz, DMSO-d_6): δ = 2.35 (d, J = 6 Hz, 4H, H_{py}), 3.36 (s, 36H, CH_3) 4.08 (br s, 8H, CH_2N), 5.00 (br s, 8H, CH_2O), 5.62 (t, J = 7 Hz, 4H, H_{py}), 6.36 (t, J = 7 Hz, 2H, H_{py}), 7.60 (br m, 4H, Hpc), 8.67 (m, 4H, H_{pc}), 8.96 ppm (m, 4H, H_{pc}); FT-IR (film): ν = 1606 (C═C), 1472 (CH_2N+), 1397 cm^{-1} (CN); UV-vis (H_2O): λ_{max} (log ε) = 263 (5.04), 313 (4.90), 633 (4.58); ESI-MS: m/z $[M - 2I]^{2+}$ calcd for $C_{62}H_{74}N_{14}O_4RuI_2$ 717.16, found: 717.17, $[M - 2I - 2py]^{2+}$ calcd for $C_{52}H_{64}N_{12}O_4RuI_2$ 638.12, found: 638.13, $[M - 3I - 2py]^{3+}$ calcd for $C_{52}H_{64}N_{12}O_4RuI$: 383.11, found: 383.12, $[M - 4I - 2py]^{4+}$ calcd for $C_{52}H_{64}N_{12}O_4Ru$ 255.51, found: 255.61.

Preparation of dendritic first generation phthalonitrile 6. To a solution of 4 (230 mg, 0.80 mmol) in CH_2Cl_2 (5 mL) was added TFA (0.37 mL, 4.80 mmol) at 0 °C. The resulting solution was allowed to warm to room temperature and monitoring of the deprotection by TLC indicated the complete removal of the Boc-protecting groups after 3 h. The acid was then neutralised by the addition of NEt_3 (0.67 mL, 4.80 mmol). Carboxylic acid **5** (425 mg, 0.97 mmol) and PyBOP (653 mg, 1.26 mmol) were added to the mixture, followed by the addition of another amount of NEt_3 (0.40 mL, 2.90 mmol) to initiate the reaction. The mixture was stirred overnight at room temperature. The

solvent was evaporated to dryness, the residue dissolved in CH_2Cl_2 and the organic phase was washed with aq. NaOH (1 M), dried with Na_2SO_4 and evaporated to dryness. Purification by column chromatography (silica gel; eluent: EtOAc/CH_2Cl_2 2 : 1) gave **6** (466 mg, 95%) as colourless foam. ^{1}H NMR (300 MHz, $CDCl_3$): δ = 1.45 (s, 18H, CH_3), 3.50 (q, J = 10.9, 5.3 Hz, 4H, CH_2N), 3.88 (q, J = 10.8, 5.3 Hz, 2H, CH_2N), 4.03 (t, J = 5.3 Hz, 4H, CH_2O), 4.26 (t, J = 5.2 Hz, 2H, CH_2O), 4.97 (br s, 2H, NH), 6.56 (br s, 1H, H_{ar}), 6.85 (br s, 1H, NH), 6.99 (br s, 2H, H_{ar}), 7.23 (dd, J = 8.8, 2.5 Hz, 1H, H_{pn}), 7.29 (d, J = 2.5 Hz, 1H, H_{pn}), 7.71 ppm (d, J = 8.8 Hz, 1H, H_{pn}); ^{13}C NMR (300 MHz, $CDCl_3$): δ = 28.4, 39.2, 39.8, 67.3, 67.7, 79.8, 104.8, 105.9, 107.5, 115.3, 115.7, 117.4, 119.3, 120.0, 135.4, 136.0, 156.1, 159.8, 161.8, 167.6 ppm; FT-IR (film): ν = 3070, 2976, 2881, 2340, 2230, 1703 cm^{-1}; high resolution ESI-MS. (MeOH): m/z $[M + Na]^+$ calcd for $C_{31}H_{39}N_5NaO_8$ 632.2802, found 632.2667.

Preparation of dendritic second generation phthalonitrile 7. To a solution of **6** (41 mg, 67.3 μmol) in CH_2Cl_2 (4 mL) was added TFA (21 μL, 269 μmol) at 0 °C. The resulting solution was allowed to warm to room temperature and monitoring of the deprotection by TLC indicated the complete removal of the Boc-protecting groups after 4 h. The acid was then neutralised through the addition of NEt_3 (38 μL, 269 μmol). Carboxylic acid **5** (88 mg, 0.20 mmol) and PyBOP (115 mg, 0.22 mmol) were added to the mixture, followed by the addition of NEt_3 (38 μL, 269 μmol) to initiate the reaction. The mixture was stirred overnight at room temperature. The solvent was evaporated to dryness, the residue dissolved in CH_2Cl_2 and the organic phase was washed with aq. NaOH (1 M), dried with Na_2SO_4 and evaporated to dryness. Purification by column chromatography (silica gel; eluent: EtOAc/CH_2Cl_2 2 : 1) gave **7** (70 mg, 83%) as colourless foam. ^{1}H NMR (300 MHz, $CDCl_3$): δ = 1.53 (s, 36H, CH_3), 3.54 (br q, 8H, CH_2N), 3.83 (br q, 4H, CH_2N), 3.93 (br q, 2H, CH_2N), 4.03 (br t, 8H, CH_2O), 4.17 (br t, 4H, CH_2O), 4.34 (br t, 2H, CH_2O), 5.39 (br s, 4H, NH), 6.55 (br s, 2H, H_{ar}), 6.60 (br s, 1H, H_{ar}), 6.96 (br s, 4H, H_{ar}), 7.09 (br s, 2H, H_{ar}), 7.23 (m, 1H, H_{pn}), 7.38 (m, 3H, H_{pn}, NH), 7.68 (d, J = 8.6 Hz, 1H, H_{pn}), 7.76 ppm (br t, 1H, H_{pn}); ^{13}C NMR (75 MHz, $CDCl_3$): δ = 21.1, 28.5, 39.4, 39.5, 39.9, 66.7, 67.3, 67.6, 79.7, 104.6, 104.9, 105.9, 107.3, 115.3, 115.7, 117.2, 119.3, 120.0, 135.3, 136.2, 136.3, 156.2, 159.8, 161.8, 167.6, 167.7 ppm. FT-IR (film): ν = 3072, 2977, 2878, 2341, 2230, 1705 cm^{-1}; high resolution MALDI-TOF MS (Dithranol): m/z $[M + Na]^+$ calcd for $C_{63}H_{83}N_9NaO_{18}$: 1276.5648, found: 1276.5759.

Preparation of zinc phthalocyanine 9. A mixture of **6** (158 mg, 0.26 mmol) and $Zn(OAc)_2$ (16 mg, 0.07 mmol) in DMAE (2 mL) was heated at reflux under an argon atmosphere overnight. The crude was poured onto water after cooling to room temperature and the resulting green precipitate was filtered, washed with MeOH and dried. Purification by column chromatography (silica gel; eluent: CH_2Cl_2/MeOH/TEA 97 : 3 : 1) and GPC (eluent: THF) afforded **9** (53 mg, 33%) as green solid. M.p.: 157–159 °C; ^{1}H NMR (300 MHz, DMSO-d_6): δ = 1.37 (s, 72H, CH_3), 3.29 (m, 16H, CH_2N), 3.64 (m, 8H, CH_2N), 3.98 (t, J = 4 Hz, 16H, CH_2O), 4.29 (t, J = 5 Hz, 8H, CH_2O), 6.63 (br s, 4H, H_{ar}), 6.91–7.05 (m, 16H, H_{ar}, NH), 7.27–7.35 (m, 8H, H_{pc}, NH), 7.72 (m, 4H, H_{pc}), 8.68 ppm (m, 4H, H_{pc}); FT-IR (film): ν = 1695 cm^{-1}; UV-vis (THF): λ_{max} (log ε) = 283 (4.8), 350 (4.9), 610 (4.5), 676 (5.2). MALDI-TOF MS (DCTB): m/z $[M]^+$ calcd for $C_{124}H_{156}N_{20}O_{32}Zn$: 2503.1, found: 2503.0.

Preparation of zinc phthalocyanine 10. A mixture of **7** (200 mg, 0.16 mmol) and $Zn(OAc)_2$ (7.3 mg, 0.04 mmol) in DMAE (2.5 mL) was heated at reflux under an argon atmosphere overnight. The crude was poured onto water after cooling to room temperature and the resulting green precipitate was filtered, washed with MeOH and dried. Purification by column chromatography (silica gel; eluent: CH_2Cl_2/MeOH/TEA 99 : 3 : 1) and GPC (eluent: THF) afforded **10** (3.2 mg, 1.6%) as a green solid. M.p.: 156–158 °C; FT-IR (film): ν (film) = 2981, 2929, 2855, 2354, 1693, 1596 cm^{-1}; MALDI-TOF MS (DCTB): m/z $[M]^+$ calcd for $ZnC_{252}H_{332}N_{36}O_{72}Zn$: 5081.3, found: 5081.4.

General procedure for preparation of ruthenium phthalocyanines 11 and 12. A solution of the appropriate phthalonitrile (4 eq.), $RuCl_3{\cdot}3H_2O$ (**11**: 1 eq., **12**: 1.2 eq.) and pyridine (8 eq.) in ethoxyethanol was deoxygenated by bubbling argon through the solution for 15 minutes. The solution was then heated at 90 °C under argon and at this temperature DBU (**11**: 4 eq., **12**: 5 eq.) was added and the mixture was heated at gentle reflux overnight. After cooling to room temperature, the crude was purified as outlined in the following text.

Preparation of ruthenium phthalocyanine 11. Prepared from **4** (200 mg, 0.696 mmol), $RuCl_3{\cdot}3H_2O$ (36 mg, 0.174 mmol) pyridine (113 μL, 1.39 mmol) and DBU (130 μl, 0.87 mmol) in ethoxyethanol (1.5 mL). The reaction mixture was poured onto water and the precipitate was filtered, washed with MeOH and dried. Purification by gradient column chromatography on silica gel (hexane/THF 4 : 1 to 1 : 1 with 1% of TEA) and GPC (eluent: THF) then afforded **11** (18 mg, 7%) as a dark blue solid. ^{1}H NMR (300 MHz, $CDCl_3$): δ = 1.53 (s, 36H, CH_3), 2.51 (d, 4H, J = 3 Hz, H_{py}), 3.79 (m, 8H, CH_2N) 4.52 (br m, 8H, CH_2O), 5.15–5.45 (br m, 8H, NH, H_{py}), 6.07 (t, J = 7 Hz, 2H, H_{py}), 7.44 (m, 4H, Hpc), 8.37–8.67 (br m, 4H, H_{pc}), 8.89 ppm (m, 4H, H_{pc}); FT-IR (film): ν = 2360 (C═N), 1716 (C═O), 1610 cm^{-1} (NHCO); UV-vis (THF): λ_{max} (log ε) = 239 (5.12), 319 (5.60), 366 (4.97), 624 (5.30); MALDI-TOF MS (DCTB): m/z $[M]^+$ calcd for $C_{70}H_{78}N_{14}O_{12}Ru$: 1408.5, found: 1408.5, $[M - 2py]^+$ calcd for $C_{60}H_{68}N_{12}O_{12}Ru$ 1250.4, found: 1250.4.

Preparation of ruthenium phthalocyanine 12. Prepared from **6** (140 mg, 0.230 mmol), $RuCl_3{\cdot}3H_2O$ (14 mg, 68.9 μmol), pyridine (37 μL, 0.459 mmol) and DBU (43 μL, 0.287 mmol) in ethoxyethanol (0.5 mL) under an argon atmosphere was refluxed overnight. After cooling to room temperature, the solvent was evaporated and the crude compound was purified by column chromatography (silica gel; eluent: hexane/THF from 4 : 1 to 1 : 1, with 1% of TEA) and GPC (eluent: THF) afforded **12** (11 mg, 7%) as a dark blue solid. M.p.: 220–221 °C; ^{1}H NMR (300 MHz, $CDCl_3$): δ = 1.44 (s, 72H, CH_3), 2.47 (d, 4H, J = 3 Hz, H_{py}), 3.50 (br s, 24H, CH_2N, NH), 4.04 (br m, 24H, CH_2N, CH_2O), 4.64 (br s, 8H, CH_2O), 5.24 (t, J = 5 Hz, 4H, H_{py}), 6.04 (t, J = 6 Hz, 2H, H_{py}), 6.56 (m, 4H, H_{ar}), 6.89–7.11 (m, 12H, H_{ar}, NH), 7.46 (m, 4H, H_{pc}), 8.64 (m, 4H,

H_{pc}), 8.97 ppm (m, 4H, H_{pc}); FT-IR (film): ν = 1743, 1645 cm^{-1}; UV-vis (THF): λ_{max} ($\log \varepsilon$) = 211 (5.7), 318 (5.4), 625 (5.0); MALDI-TOF MS (DCTB): m/z $[M - py]^+$ calcd for $C_{129}H_{161}N_{21}O_{32}Ru$: 2618.1, found: 2617.9.

General procedure for quaternization of Boc-appended Pcs. Step (i): The appropriate Boc-protected Pc (1 eq.) was dissolved in CH_2Cl_2 and the solution was cooled to 0 °C. TFA (10 eq. per Boc group) was added and the mixture was stirred for 1 h at room temperature until complete Boc deprotection. All volatiles were removed under reduced pressure. Step (ii): The crude was dissolved in DMF, PMP (1–2 eq. per original Boc group) and an excess of CH_3I (5–10 eq. per original Boc group) were added and the reaction was allowed to stir overnight at room temperature. The addition of acetone induced precipitation of the quaternary ammonium salts, which are purified by several cycles of sonication and washing with acetone and a mixture of acetone containing DMF (6%).

Preparation of polycationic ZnPc. Step (i): Prepared from **8** (50 mg, 41 μmol) and TFA (126 μL, 1.65 mmol) in CH_2Cl_2 (0.3 mL) after 4 h at room temperature. Step (ii): PMP (30 μL, 0.16 mmol) and CH_3I (30 μL, 0.456 mmol) in DMF (0.3 mL). The workup as described in the general procedure yielded **ZnPc** (60 mg, 98%) as a green solid. The characterisation data confirmed the literature values.[42,43]

Preparation of polycationic ZnPc1. Step (i): Prepared from **9** (17 mg, 6.79 μmol) and TFA (42 μL, 0.543 mmol) in CH_2Cl_2 (1 mL) after 7 h at room temperature. Step (ii): PMP (20 μL, 109 μmol) and CH_3I (34 μL, 0.543 mmol) in DMF (0.2 mL). The workup as described in the general procedure yielded **ZnPc1** (17 mg, 96%) as a green solid. M.p.: >250 °C; ^{1}H NMR (300 MHz, DMSO-d_6): δ = 3.22 (s, 72H, CH_3), 3.83 (br s, 16H, CH_2N), 3.98 (br s, 8H, CH_2N), 4.56 (br s, 16H, CH_2O), 4.76 (br s, 8H, CH_2O), 6.88 (br s, 4H, H_{ar}), 7.19 (br s, 4H, NH), 7.31 (br s, 8H, H_{ar}), 7.84 (m, 4H, H_{pc}), 8.97 (m, 4H, H_{pc}), 9.35 (m, 4H, H_{pc}); FT-IR (film): ν = 1590 cm^{-1}; UV-vis (H_2O): λ_{max} ($\log \varepsilon$) = 286 (4.56), 347 (4.67), 629 (4.4), 690 (4.85); ESI-MS (MeOH): m/z $[M - 3I^-]^{3+}$ calcd for $C_{108}H_{148}N_{20}O_{16}ZnI_5$: 893.86, found: 893.86, $[M - 4I^-]^{4+}$ calcd for $C_{108}H_{148}N_{20}O_{16}ZnI_4$: 638.67, found: 638.68.

Preparation of polycationic RuPc. Step (i): Prepared from **11** (30 mg, 21.3 μmol) and TFA (65 μL, 0.852 mmol) in CH_2Cl_2 (0.3 mL) after 4 h at room temperature. Step (ii): PMP (15 μL, 85.2 μmol) and CH_3I (52 μL, 0.852 mmol) in DMF (0.3 mL). The workup as described in the general procedure yielded **RuPc** (31 mg, 85%) as a dark blue solid. For characterization data see above.

Preparation of polycationic RuPc1. Step (i): Prepared from **12** (25 mg, 9.27 μmol) and TFA (28 μL, 0.371 mmol) in CH_2Cl_2 (1 mL) after 4 h at room temperature. Step (ii) PMP (27 μL, 148 μmol) and CH_3I (23 μL, 0.371 mmol) in DMF (0.5 mL). The workup as described in the general procedure yielded **RuPc1** (21 mg, 82%) as a dark blue solid. M.p.: >250 °C; ^{1}H NMR (300 MHz, DMSO-d_6): δ = 2.35 (d, 4H, J = 4 Hz, H_{py}), 3.12 (s, 72H, CH_3), 3.74–3.95 (br m, 24H, CH_2N, CH_2O), 4.46–4.70 (br m, 24H, CH_2N, CH_2O), 5.60 (t, J = 5 Hz, 4H, H_{py}), 6.35 (t, J = 6 Hz, 2H, H_{py}), 6.88 (br s, 4H, H_{ar}), 7.14–7.35 (m, 8H, H_{ar}), 7.53 (m, 4H, H_{pc}), 8.59 (m, 4H, H_{pc}), 8.76–9.02 (m, 8H, H_{pc}, NH); FT-IR (film): ν = 2360, 1594 cm^{-1}; UV-vis (H_2O): λ_{max} ($\log \varepsilon$) = 260 (5.05), 309 (4.7), 635 (4.3).

General spectroscopic measurements

Steady-state characterisation. All spectroscopic measurements were carried out in 1 cm quartz cuvettes (Hellma, Germany) in air-saturated solutions at rt. Absorption spectra were recorded with a double-beam Cary 6000i spectrophotometer (Varian, Palo Alto, CA). Fluorescence emission spectra were recorded by means of a Spex Fluoromax-4 spectrofluorometer (Horiba Jobin-Ybon, Edison, NJ). The absolute fluorescence quantum yield (Φ_F) was calculated using eqn (1).

$$\Phi_{F,sample} = \left(\frac{I_{sample}}{I_{reference}}\right)\cdot\left(\frac{\eta_{sample}{}^2}{\eta_{reference}{}^2}\right)\Phi_{F,reference} \quad (1)$$

where I_x corresponds to the fluorescence intensity, integrated over the entire emission spectra and corrected by differences in the absorption ($1–10^{-Abs}$) for the sample and reference, respectively. All solutions were set below 0.1 absorbance value at the excitation wavelength. η_i stands for the refractive index of the sample and reference solutions.

Singlet oxygen measurements. Near infrared (NIR) phosphorescence of $^1O_2$ was detected by means of a customised PicoQuant Fluotime 200 system.[63] A diode-pumped pulsed Nd:YAG laser (FTSS355-Q; Crystal Laser, Berlin, Germany) working at 1 kHz repetition rate (1.2 μJ per pulse, 1 ns pulse-width) was used for excitation either at 355 or 532 nm. A 1064 nm rugate notch filter (Edmund Optics Ltd, York, UK) was placed in the laser path to remove any NIR emission. The luminescence exiting from the side of the sample was collected at 90 degrees, filtered by using a 1100 nm long-pass filter (Edmund Optics Ltd, York, UK) and a narrow bandpass filter at 1275 nm (bk-1270-70-B, bk Interferenzoptik, Germany) to isolate the NIR phosphorescence. A TE-cooled NIR-sensitive photomultiplier tube assembly (H9170-45; Hamamatsu Photonics, Hamamatsu City, Japan) coupled with a multichannel scaler (Nanoharp 250, PicoQuant Gmbh, Germany) was used as the photon-counting detector. GraphPad Prism 5 data analysis software was used to fit the singlet oxygen time-resolved luminescence decays, $S(t)$, according to eqn (2).

$$S(t) = S_0 \times \frac{\tau_\Delta}{\tau_\Delta - \tau_T} \times \left(e^{-t/\tau_\Delta} - e^{-t/\tau_T}\right) \quad (2)$$

S_0 is defined as a quantity proportional to Φ_Δ. In order to assess the Φ_Δ value of the different dendrimeric Pcs, optically-matched solutions of the dendrimeric PSs and the appropriate references (see Table 1) were excited and their S_0 values were scaled using eqn (3).

$$\Phi_{\Delta,sample} = \Phi_{\Delta,ref} \times \frac{S_{0,sample}}{S_{0,reference}} \quad (3)$$

Microbial studies

Microbial strains and culture conditions. *Escherichia coli* CECT 101 and *Staphylococcus aureus* CECT 239 were obtained

from the Spanish Type Culture Collection (CECT, Valencia, Spain). *Candida albicans* ATCC 18804 was purchased from LGC Promochem (Teddington, UK). Bacterial cells were grown overnight in sterile tryptic soy broth (TSB) at 37 °C and then subcultured in fresh TSB at the same temperature in an orbital shaking incubator until the required optical density was obtained. *C. albicans* cultures were grown in a similar fashion, using Sabouraud broth as the growing medium and 35 °C as temperature to an optical density of 0.7 at 600 nm (corresponding to approx. 10^7 CFU mL^{-1}).

Photodynamic inactivation studies. Subcultured cell suspensions were grown to an exponential phase, then centrifuged (5 min, 3500 rpm), suspended and adjusted in PBS to an optical density at 600 nm to achieve approx. 10^8 CFU mL^{-1}. Cell suspensions in PBS were incubated in the dark at rt. for 30 min with the appropriate Pc concentration. Then, bacterial suspension aliquots were placed in 96-well plates. The wells were illuminated from the top of the plates by means of a LED-lamp (Sorisa Photocare; 635 ± 15 nm). The fluence rates were routinely measured using a power meter. At the time points when the desired fluence had been obtained, aliquots were thoroughly mixed before sampling to avoid bacteria settlement. Controlling the cell irradiation without PS was also performed to exclude any inactivation due to light or heating effects. For the determination of population reduction, aliquots were serially diluted, streaked on nutrient agar plates, and incubated in the dark at the appropriate temperature.

Conflicts of interest

There are no conflicts to declare.

Acknowledgements

This work was supported by the Spanish Ministerio de Economía y Competitividad (grants CTQ2013-48767-C3-1-R, CTQ2014-52869-P and CTQ2016-78454-C2-1-R) and the Comunidad de Madrid (FOTOCARBON, S2013/MIT-2841). F. S. thanks the Universidad Autónoma de Madrid, Spain for a PhD fellowship FPI-UAM.

References

1 T. G. St Denis, T. Dai, L. Izikson, C. Astrakas, R. R. Anderson, M. R. Hamblin and G. P. Tegos, *Virulence*, 2011, **2**, 509–520.
2 G. J. Alangaden, *Infect. Dis. Clin. North Am.*, 2011, **25**, 201–225.
3 D. M. Sievert, P. Ricks, J. R. Edwards, A. Schneider, J. Patel, A. Srinivasan, A. Kallen, B. Limbago and S. Fridkin, *Infect. Control Hosp. Epidemiol.*, 2013, **34**, 1–14.
4 World Health Organization, *Antimicrobial resistance: global report on surveillance*, 2014.
5 I. Roca, M. Akova, F. Baquero, J. Carlet, M. Cavaleri, S. Coenen, J. Cohen, D. Findlay, I. Gyssens, O. E. Heure, G. Kahlmeter, H. Kruse, R. Laxminarayan, E. Liébana, L. López-Cerero, A. MacGowan, M. Martins, J. Rodríguez-Baño, J. M. Rolain, C. Segovia, B. Sigauque, E. Taconelli, E. Wellington and J. Vila, *New Microbes New Infect.*, 2015, **6**, 22–29.
6 Z. A. Qureshi, L. E. Hittle, J. A. O. Hara and J. I. Rivera, *Clin. Infect. Dis.*, 2015, **60**, 1295–1303.
7 H. W. Boucher, G. H. Talbot, J. S. Bradley, J. E. Edwards, D. Gilbert, L. B. Rice, M. Scheld, B. Spellberg and J. Bartlett, *Clin. Infect. Dis.*, 2009, **48**, 1–12.
8 A. Teillant, S. Gandra, D. Barter, D. Morgan and R. Laxminarayan, *Lancet Infect. Dis.*, 2015, **15**, 1421437.
9 L. D. Högberg, A. Heddini and O. Cars, *Trends Pharmacol. Sci.*, 2010, **31**, 509–515.
10 L. J. V. Piddock, *Lancet Infect. Dis.*, 2012, **12**, 249–253.
11 K. Bush, *Curr. Opin. Pharmacol.*, 2012, **12**, 527–534.
12 B. Spellberg, M. Blaser, R. J. Guidos, H. W. Boucher, J. S. Bradley, B. I. Eisenstein, D. Gerding, R. Lynfield, L. B. Reller, J. Rex, D. Schwartz, E. Septimus, F. C. Tenover and D. N. Gilbert, *Clin. Infect. Dis.*, 2011, **52**, S397–S428.
13 E. M. M. Quigley, *Curr. Opin. Pharmacol.*, 2011, **11**, 593–603.
14 E. Kutter, D. De Vos, G. Gvasalia, Z. Alavidze, L. Gogokhia, S. Kuhl and S. T. Abedon, *Curr. Pharm. Biotechnol.*, 2010, **11**, 69–86.
15 B. M. Peters, M. E. Shirtliff and M. A. Jabra-Rizk, *PLoS Pathog.*, 2010, **6**, e1001067.
16 B. M. Peters, M. A. Jabra-Rizk, G. A. O'May, J. W. Costerton and M. E. Shirtliff, *Clin. Microbiol. Rev.*, 2012, **25**, 193–213.
17 P. D. Cotter, R. P. Ross and C. Hill, *Nat. Rev. Microbiol.*, 2013, **11**, 95–105.
18 M. M. Pettigrew, J. K. Johnson and A. D. Harris, *Ann. Epidemiol.*, 2016, **26**, 342–347.
19 E. E. Gill, O. L. Franco and R. E. W. Hancock, *Chem. Biol. Drug Des.*, 2015, **85**, 56–78.
20 M. R. Hamblin and T. Hasan, *Photochem. Photobiol. Sci.*, 2004, **3**, 436–450.
21 T. Dai, Y. Y. Huang and M. R. Hamblin, *Photodiagn. Photodyn. Ther.*, 2009, **6**, 170–188.
22 M. Wainwright, T. Maisch, S. Nonell, K. Plaetzer, A. Almeida, G. P. Tegos and M. R. Hamblin, *Lancet*, 2017, **2**, e49–e55.
23 C. G. Claessens, U. Hahn and T. Torres, *Chem. Rec.*, 2008, **8**, 75–97.
24 G. de la Tore, G. Bottari, U. Hahn and T. Torres, *Functional phthalocyanine molecular materials*, Springer Berlin Heidelberg, Berlin, Heidelberg, 2010, vol. 135.
25 G. Bottari, G. de la Torre, D. M. Guldi and T. Torres, *Chem. Rev.*, 2010, **110**, 6768–6816.
26 A. B. Sorokin, *Chem. Rev.*, 2013, **113**, 8152–8191.
27 H. Yoshiyama, N. Shibata, T. Sato, S. Nakamura and T. Toru, *Org. Biomol. Chem.*, 2009, **7**, 2265–2269.
28 Y. Li, J. Wang, X. Zhang, W. Guo, F. Li, M. Yu, X. Kong, W. Wu and Z. Hong, *Org. Biomol. Chem.*, 2015, **13**, 7681–7694.

29 F. Li, Q. Liu, Z. Liang, J. Wang, M. Pang, W. Huang, W. Wu and Z. Hong, *Org. Biomol. Chem.*, 2016, **14**, 3409–3422.
30 L. Luan, W. Fang, W. Liu, M. Tian, Y. Ni, X. Chen and X. Yu, *Org. Biomol. Chem.*, 2016, **14**, 2985–2992.
31 P.-C. Lo, J.-D. Huang, D. Y. Y. Cheng, E. Y. M. Chan, W.-P. Fong, W.-H. Ko and D. K. P. Ng, *Chem. – Eur. J.*, 2004, **10**, 4831–4838.
32 S. Tuncel, J. Fournier-dit-Chabert, F. Albrieux, V. Ahsen, S. Ducki and F. Dumoulin, *Org. Biomol. Chem.*, 2012, **10**, 1154–1157.
33 C. M. Allen, W. M. Sharman and J. E. Van Lier, *J. Porphyrins Phthalocyanines*, 2001, **5**, 161–169.
34 A. B. Ormond and H. S. Freeman, *Materials*, 2013, **6**, 817–840.
35 U. Hahn, F. Setaro, X. Ragàs, A. Grey-Weale, S. Nonell and T. Torres, *Phys. Chem. Chem. Phys.*, 2010, **12**, 1–9.
36 F. Figueira, P. M. R. Pereira, S. Silva, J. A. S. Cavaleiro and J. P. C. Tome, *Curr. Org. Synth.*, 2014, **11**, 110–126.
37 W. S. Li and T. Aida, *Chem. Rev.*, 2009, **109**, 6047–6076.
38 F. Setaro, R. Ruiz-González, S. Nonell, U. Hahn and T. Torres, *J. Inorg. Biochem.*, 2014, **136**, 170–176.
39 F. Setaro, R. Ruiz-González, S. Nonell, U. Hahn and T. Torres, *J. Porphyrins Phthalocyanines*, 2016, **20**, 1–10.
40 F. Setaro, M. Brasch, U. Hahn, M. S. T. Koay, J. J. L. M. Cornelissen, A. de la Escosura and T. Torres, *Nano Lett.*, 2015, **15**, 1245–1251.
41 E. Anaya-Plaza, E. van de Winckel, J. Mikkilä, J.-M. Malho, O. Ikkala, O. Gulías, R. Bresolí-Obach, M. Agut, S. Nonell, T. Torres, M. A. Kostiainen and A. de la Escosura, *Chem. – Eur. J.*, 2017, **23**, 4320–4326.
42 L. Zhang, J. Huang, L. Ren, M. Bai, L. Wu, B. Zhai and X. Zhou, *Bioorg. Med. Chem.*, 2008, **16**, 303–312.
43 J. Marino, M. C. García Vior, L. E. Dicelio, L. P. Roguin and J. Awruch, *Eur. J. Med. Chem.*, 2010, **45**, 4129–4139.
44 S. Fukuzumi, K. Ohkubo, J. Ortiz, A. M. Gutiérrez, F. Fernández-Lázaro and A. Sastre-Santos, *J. Phys. Chem. A*, 2008, **112**, 10744–10752.
45 S. J. E. Mulders, A. J. Brouwer, P. G. J. van der Meer and R. M. J. Liskamp, *Tetrahedron Lett.*, 1997, **38**, 631–634.
46 A. J. Brouwer, S. J. E. Mulders and R. M. J. Liskamp, *Eur. J. Org. Chem.*, 2001, 1903–1915.
47 M. Sibrian-Vazquez, J. Ortiz, I. V. Nesterova, F. Fernandez-Lazaro, A. Sastre-Santos, S. A. Soper and M. G. H. Vicente, *Bioconjugate Chem.*, 2007, **18**, 410–420.
48 H. Z. Sommer, H. I. Lipp and L. L. Jackson, *J. Org. Chem.*, 1971, **36**, 824–828.
49 A. A. Gorman and M. A. J. Rodgers, in *Handbook of organic photochemistry*, ed. J. C. Scaiano, CRC Press, Boca Raton, 1989, vol. II, pp. 229–247.
50 S. L. Murov, I. Carmichael and G. L. Hug, *Handbook of Photochemistry*, CRC Press, 2nd edn, 1993, vol. 2.
51 R. W. Redmond and J. N. Gamlin, *Photochem. Photobiol.*, 1999, **70**, 391–475.
52 E. Reddi, M. Ceccon, G. Valduga, G. Jori, J. C. Bommer, F. Elisei, L. Latterini and U. Mazzucato, *Photochem. Photobiol.*, 2002, **75**, 462–470.
53 G. P. Tegos, T. N. Demidova, D. Arcila-Lopez, H. Lee, T. Wharton, H. Gali and M. R. Hamblin, *Chem. Biol.*, 2005, **12**, 1127–1135.
54 M. P. Cormick, M. G. Alvarez, M. Rovera and E. N. Durantini, *Eur. J. Med. Chem.*, 2009, **44**, 1592–1599.
55 L. Huang, Y. Y. Huang, P. Mroz, G. P. Tegos, T. Zhiyentayev, S. K. Sharma, Z. Lu, T. Balasubramanian, M. Krayer, C. Ruzie, E. Yang, H. L. Kee, C. Kirmaier, J. R. Diers, D. F. Bocian, D. Holten, J. S. Lindsey and M. R. Hamblin, *Antimicrob. Agents Chemother.*, 2010, **54**, 3834–3841.
56 X. Ragàs, D. Sánchez-García, R. Ruiz-González, T. Dai, M. Agut, M. R. Hamblin and S. Nonell, *J. Med. Chem.*, 2010, **53**, 7796–7803.
57 T. N. Demidova and M. R. Hamblin, *Antimicrob. Agents Chemother.*, 2005, **49**, 2329–2335.
58 F. Li, M. Feterl, Y. Mulyana, J. M. Warner, J. G. Collins and F. R. Keene, *J. Antimicrob. Chemother.*, 2012, **67**, 2686–2695.
59 M. Merchat, G. Bertolini, P. Giacomini, A. Villanueva and G. Jori, *J. Photochem. Photobiol., B*, 1996, **32**, 153–157.
60 D. A. Caminos, M. B. Spesia and E. N. Durantini, *Photochem. Photobiol. Sci.*, 2006, **5**, 56–65.
61 E. Alves, L. Costa, C. M. B. Carvalho, J. P. C. Tomé, M. A. Faustino, M. G. Neves, A. C. Tomé, J. A. Cavaleiro, A. Cunha and A. Almeida, *BMC Microbiol.*, 2009, **9**, 1–13.
62 R. Ruiz-González, M. Agut, E. Reddi and S. Nonell, *Int. J. Mol. Sci.*, 2015, **16**, 27072–27086.
63 A. Jiménez-Banzo, X. Ragàs, P. Kapusta and S. Nonell, *Photochem. Photobiol. Sci.*, 2008, **7**, 1003–1010.